Article:
Thorp-Greenwood, FL, Pritchard, VE, Coogan, MP et al. (1 more author) (2016) Tris(rhenium fac-tricarbonyl) Polypyridine Functionalized Cyclotriguaiacylene Ligands with Rich and Varied Emission. Organometallics, 35 (11). pp. 1632-1642. ISSN 0276-7333

https://doi.org/10.1021/acs.organomet.6b00099

Tris-rhenium fac-tricarbonyl polypyridine-functionalised cyclotriguaiacylene ligands with rich and varied emission.

Flora L. Thorp-Greenwood,[a‡] *Victoria E. Pritchard,*[a‡] *Michael P. Coogan* [b*] *and Michaele J. Hardie*[a]*

a School of Chemistry, University of Leeds, Leeds, West Yorkshire, LS2 9JT.

b Department of Chemistry, Lancaster University, Bailrigg, Lancaster, LA1 4YB, United Kingdom.

‡ Joint first authors

Keywords Rhenium, Cyclotriveratrylene, Trinuclear complex, Luminescence, Dual-emission.

Abstract

Trinuclear rhenium fac-tricarbonylbromide complexes have been synthesized coordinated to the host molecules tris(4-[4-methyl-2,2’-bipyridyl]methyl)cyclotriguaiacylene (L1), tris(4-[4-methyl-2,2’-bipyridoyl])cyclotriguaiacylene (L2), or tris(4-[2,2',6',2"-terpyridyl]benzyl)

cyclotriguaiacylene (L3) ligands. The structure of L1 and complexes [{$Re(CO)_3Br$}$_3$(L1)] **1** and [{$Re(CO)_3Br$}$_3$(L3)] **3** have been elucidated through X-ray single-crystal diffraction, with complex **3** crystallizing as a conglomerate. The steady-state luminescent properties and time resolved fluorescence studies of the complexes have been conducted and revealed an unusual dual-emission phenomenon for complex **2**. Complexes **1** and **2** show red-shifted emission wavelengths compared with those typical of monometallic $Re(CO)_3$-bipy-Br complexes, while complex **3** showed an unusual excitation-dependent variation of emission wavelength.

Introduction

Cyclotriguaiacylene (CTG) is a chiral rigid crown-shaped macrocycle with a hydrophobic cavity [1] analogous to the achiral cyclic host molecule cyclotriveratrylene (CTV), Chart 1. CTV and its analogues may act as a molecular host, binding guest molecules in a non-covalent fashion,[2] with a particular affinity for binding fullerenes.[3] CTG can be functionalised at the upper rim through its hydroxyl substituents to give tripodal bowl-shaped ligands capable of binding three metal centres.[2] Examples of such trinuclear transition metal complexes of CTV-type ligands include Cu(II/I) complexes of hexakis(2,2'-bipyridylmethyl)cyclotriveratrylene which act as conformational switches,[4] anion-binding ferrocene-appended derivatives of CTV,[5] Ni(II) complexes of salicylaldiminato derivatives of CTV,[6] a $CuCl_2$ complex of tris(4-[2,2',6',2''-terpyridyl]benzyl)cyclotriguaiacylene (ligand L3 in this study),[7] Pd(II) and Cu(II) complexes of hexakis(2-pyridylmethyl)cyclotriveratrylene,[8] and a Cu(I) complex of a tris(2-pyridylmethyl)-amine decorated CTG which forms adducts with O_2 and other small molecules.[9] CTV itself can also behave as an organometallic ligand to form trinuclear complexes by binding metals through its arene faces.[10]

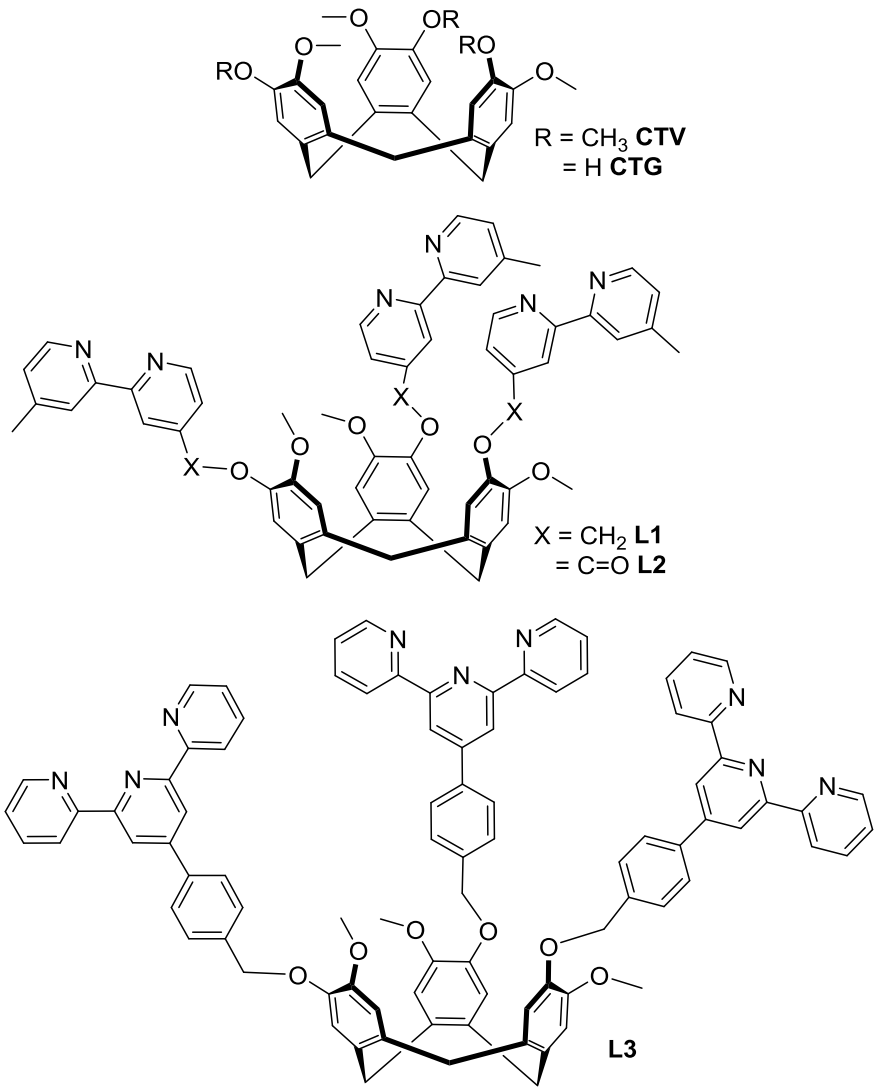

Chart 1

In this study, we investigate *tris*-(bromo-*fac*-tricarbonylrhenium(I)) complexes of CTG ligands decorated with chelating NN donor groups, namely (±)-tris(4-[4-methyl-2,2'-bipyridyl]methyl)-cyclotriguaiacylene (L1), (±)-tris(4-[4-methyl-2,2'-bipyridoyl])-cyclotriguaiacylene (L2), and (±)-tris(4-[2,2',6',2''-terpyridyl]benzyl)cyclotriguaiacylene (L3), Chart 1. Rhenium carbonyl complexes are of interest as complexes of the type $[Re(CO)_3(NN)X]$, where NN is a bisimine moiety and X = halide, are well known to display interesting photochemical and photophysical

behaviors,[11] and there is considerable precedent for rhenium-based luminescence detection of host-guest binding.[12,13] They may exhibit long wavelength emission and large Stokes shifts which are advantageous properties for lumophores and sensors, particularly in the biomedical imaging field.[14] Long wavelengths allow larger samples to be examined, with NIR emitters showing the highest degree of, and least damaging, tissue-penetration,[15] and easy discrimination from superfluous, high energy auto-fluorescence from endogenous tissues. Additionally long luminescence lifetimes are attractive, as auto-fluorescence can be excluded from the recorded emission profile using time resolved emission spectroscopy (TRES)[16] or fluorescence lifetime imaging microscopy (FLIM).[17]

Tris-(bromo-*fac*-tricarbonylrhenium(I)) complexes of CTG-type ligands are therefore attractive candidates for the development of luminescence sensing agents given: their potential for attractive physical properties as outlined above; the ability of CTGs to act as hosts; and the precedent for rhenium based luminescence detection of host-guest binding. Furthermore, the availability of L1-L3 allows us to investigate how changes in conjugation of the ligand affect not only the photophysical properties of the trinuclear complexes, but also their solubility and hence their potential in luminescent sensing applications. While there are no previous examples of $Re(CO)_3X$ moieties being appended to CTV-type host molecules, there are a number of reports of other classes of macrocyclic host molecules being decorated in this fashion. For example, decoration of calixarenes with $[Re(CO)_3X(bpy)$ (Bpy = 2,2'-bipyridyl) groups at the upper [18,19] or lower calixarene rim [20,21] have been reported, and includes cases of complexes showing luminescence sensing behavior for fullerenes [18] or anions.[20] The $Re(CO)_3Br$ unit has also been employed as a building tecton to link pyridyl appended cavitands into ditopic cavitand assemblies,[22] and as metallobridges to stabilize the extended cavity of an expanded

calix[4]arene.[23] In related work, the fac-$Re(CO)_3$ unit has been used to build a variety of metallacyclic, metallacage or metallacavitand complexes.[13,24]

Results and Discussion

The ligands (±)-tris(4-[4-methyl-2,2'-bipyridyl]methyl)-cyclotriguaiacylene (L1) [25] and (±)-tris(4-[2,2',6',2''-terpyridyl]benzyl)cyclotriguaiacylene (L3) [7] have been previously reported. Ligand (±)-tris(4-[4-methyl-2,2'-bipyridoyl])-cyclotriguaiacylene (L2) was prepared according to Scheme 1. 4-Methyl-4'-carboxybipyridine was treated with thionyl chloride to give the corresponding acid chloride, an excess of which was reacted *in situ* with CTG to give a racemic mixture of L2 in 76 % yield on work-up. The trinuclear complexes [{$Re(CO)_3Br$}$_3$(L1)] **1**, [{$Re(CO)_3Br$}$_3$(L2)] **2** and [{$Re(CO)_3Br$}$_3$(L3)] **3** were synthesized from reaction of the appropriate cavitand ligand with slightly over three equivalents of $Re(CO)_5Br$, as is indicated for complex **2** in Scheme 1. The three complexes were isolated as yellow polycrystalline solids in high yields. Complexes **1** and **2** showed moderate solubility in organic solvents such as $MeNO_2$ and acetone with much higher solubility in dimethylsulfoxide (DMSO). Complex **3** was sparingly soluble in chlorinated solvents but showed better solubility in DMSO.

Complexes were characterized by ES-MS and NMR. Mass spectra typically showed the presence of the $[Re(CO)_3Br_3(L)_2]\cdot H^+$ and/or the $[Re(CO)_3Br_2(L)_2]^+$ species with the loss of one Br^- ligand, sometimes as a solvate, and all with characteristic isotope patterns (see Figures S10, S16, S21, supporting information). The ^{1}H NMR spectra of complexes **1** - **2** indicate that, in solution, the trinuclear Re complexes retain the C_3 symmetry of the cavitand ligands, with coordination induced shifts observed for bipyridine protons and peak broadening observed in both cases (see Figures S6 and S12 supporting information). The ^{1}H NMR spectrum of complex **3** is more

complicated, see Figure S18 supporting information. The cyclotriguaiacylene-core retains C_3-symmetry and the usual bowl-conformation as exemplified by the two doublets corresponding to the endo and exo lower rim CTG–CH_2- protons at 4.69 and 3.48 ppm respectively, and singlets at 7.01 and 7.17 ppm attributed to the two arene CTG protons. The remainder of the aromatic region integrates to the expected number of protons, however contains more peaks than just for ligand L3 alone. This is typical of [$Re(CO)_3X$(terpy)] complexes and demonstrates bidentate NN rather than tridentate NNN coordination of the ligand to Re, furthermore such complexes show fluxionality of the coordinated and uncoordinated pyridyl groups.[26] The low solubility of complex **3** in solvents other than DMSO precludes low temperature NMR studies to fully investigate this here.

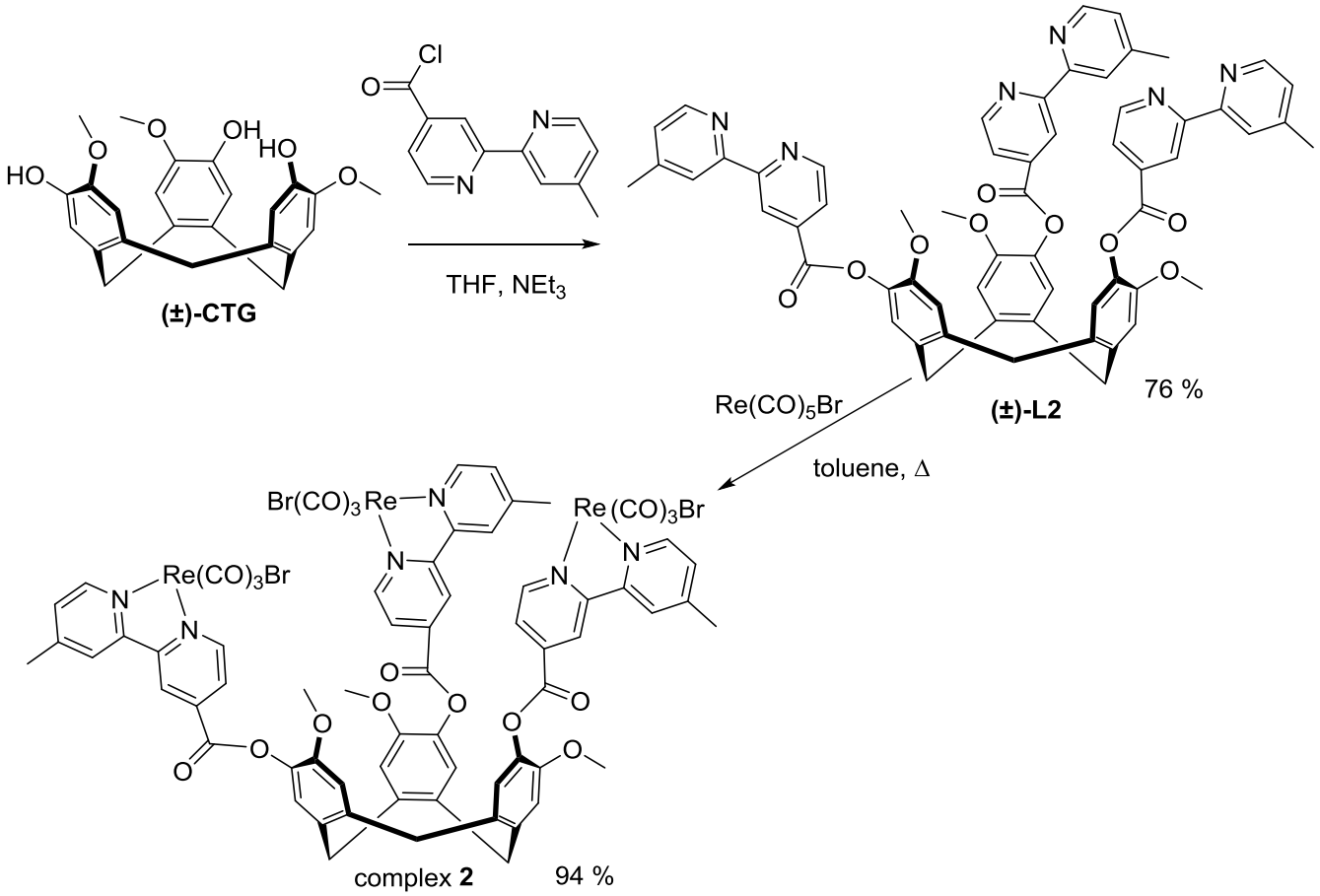

Scheme 1: Synthetic route for the preparation of L2 and complexation with $Re(CO)_5Br$ to form complex **2**. Complexes **1** and **3** were synthesized in an analogous fashion from ligands L1 and L3 respectively.

Single crystals suitable for X-ray structure determination were obtained for complexes **1** and **3** by vapor diffusion of diethyl ether into a $MeNO_2$ solution of **1** and on standing a saturated solution of **3** in DMSO for several months. Single crystals of a clathrate complex of ligand L1, L1·(Et_2O), were also obtained by vapour diffusion of diethylether into a chloroform solution of L1. The structure of L1·(Et_2O) was solved in the orthorhombic space group Pbna and has one L1

and one molecule of diethyl ether in the asymmetric unit. The ligand structure does not have C_3 symmetry, with each bipyridine arm crystallographically distinct with torsion angles along the ether linkage between 48.9° and 53.5°, Figure 1a. The ligand molecule crystallises with a 'bowl-in-bowl' stacking motif, with alternating ligand enantiomers forming an infinite stack, Figure 1b. Bowl-in-bowl stacking motifs in clathrate complexes are relatively common for both the parent CTV [27] (albeit in a slightly tilted fashion) and for upper rim functionalized analogues.[28] Neighboring stacks display an alternating head-up/head-down motif with solvent diethyl ether molecules contained within the resulting channels, leading to the formation of a clathrate complex (see Supporting information, Figure S24).

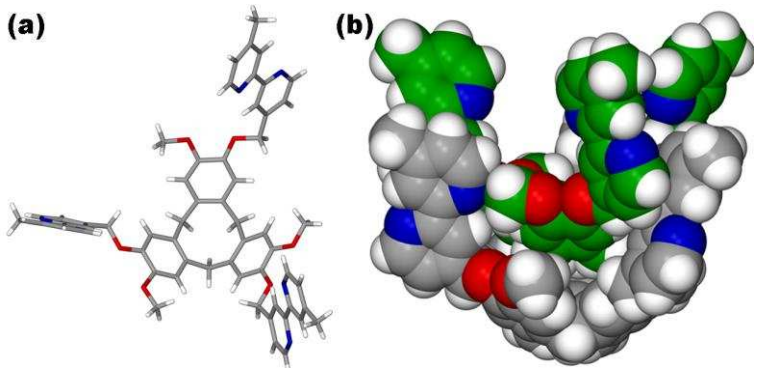

Figure 1: From the X-ray crystal structure of the clathrate complex L1·(Et_2O). (a) Ligand L1; (b) bowl-in-bowl stacking of ligand enantiomers.

The crystal structure of complex [{$Re(CO)_3Br$}$_3$(L1)]·n(CH_3NO_2) **(**= (**1**)·n(CH_3NO_2)) was solved in the centro-symmetric space group R-3. There are two crystallograpically distinct complex **1** molecules in the crystal structure, each with one third of a complex in the asymmetric unit. One nitromethane molecule per asymmetric unit could be located, however the actual level of

solvation is likely to be higher than this. Both types of [{$Re(CO)_3Br$}$_3$(L1)] have crystallographic C_3 symmetry with a 3-fold rotational axis centered in the middle of the CTG cavitand bowl, and are distinguished by relative positioning of the Br ligands and torsion angles between the core cavitand and bpy (=2,2'-bipyridine) fragments. As anticipated, the Re(I) cations have approximately octahedral coordination with a fac arrangement of CO ligands (Re-C distances between 1.862(16) and 2.04(2) Å), chelating bpy moiety (Re-N distances between 2.170(13) and 2.221(14) Å) and Br ligand arranged cis to the bpy (Re-Br distances 2.587(2) and 2.597(2) Å). For one [{$Re(CO)_3Br$}$_3$(L1)], complex A in Figure 2a, the Br^- ligands are oriented away from the cavitand bowl and the core arene and bpy arm are nearly coplanar with a C_{arene}-O-CH_2-C_{bpy} torsion angle of -177.2°. In complex B (Figure 2b) the Br^- ligands are oriented towards the cavitand bowl, and Re(bpy) fragment is rotated away with the C_{arene}-O-CH_2-C_{bpy} torsion angle at 165.1°. Re…Re distances in type A are 17.4 Å, whereas they are 20.8 Å in type B, giving type B a shallower cavitand bowl.

In the crystal lattice of **1**·n(CH_3NO_2) the [{$Re(CO)_3Br$}$_3$(L1)] complexes adopt a bowl-in-bowl stacking motif similar to that seen in the ligand clathrate complex L1·(Et_2O). Unlike in L1·(Et_2O), however, the bowl-in-bowl stacks occur in a pairwise fashion and do not extend into infinite stacks. Each pair of bowl-in-bowl stacked [{$Re(CO)_3Br$}$_3$(L1)] complexes is racemic with a type A complex with one ligand enantiomer and a type B complex with the opposite enantiomer, Figure 2c. The distances between the cavitands in these bowl-in-bowl stacks for L1·(Et_2O) and **1**·n(CH_3NO_2) are nearly identical at 4.67 and 4.71 Å respectively as measured between the center of the C atoms of the {-(CH_2)-}$_3$ lower rim of L1. The open bowl of each [{$Re(CO)_3Br$}$_3$(L1)] bowl-in-bowl pair is capped by interdigitating {$Re(CO)_3Br$(bpy)} moieties

in opposite bowl-down orientation above their plane, Figure 3. Despite the multitude of aromatic rings, there is no evidence of significant π-π stacking interactions within **1**·n(CH_3NO_2).

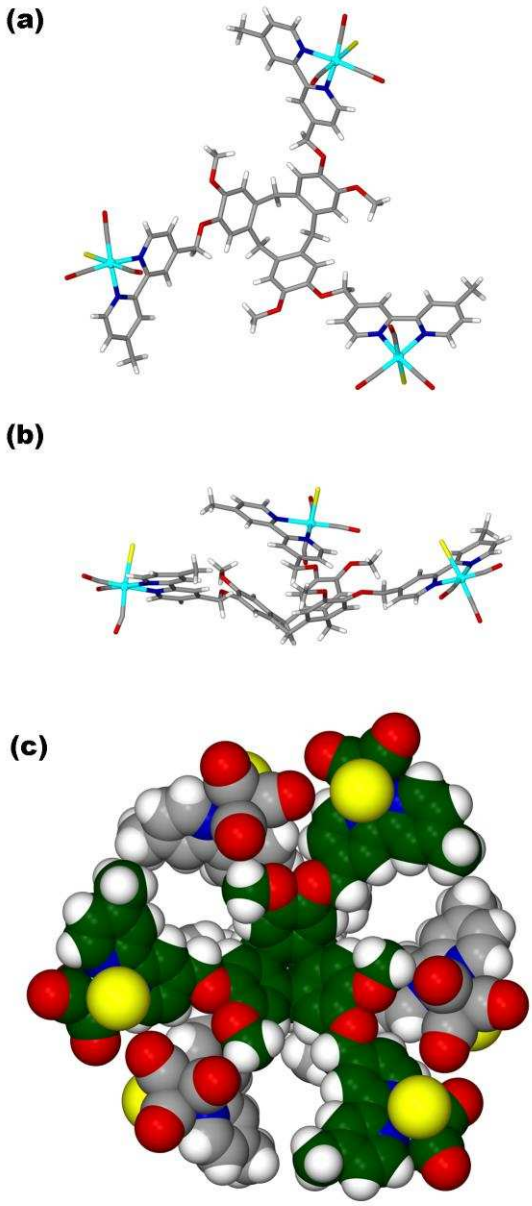

Figure 2: From the X-ray crystal structure of the complex **1**·n(CH_3NO_2). (a) Type A [{$Re(CO)_3Br$}$_3$(L1)] ; (b) type B [{$Re(CO)_3Br$}$_3$(L1)]; (c) bowl-in-bowl stacking of type A and B to form a pair.

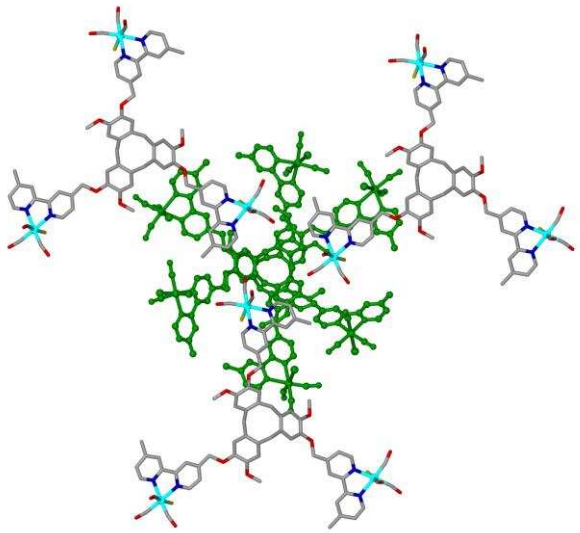

Figure 3. Partial packing diagram for complex **1**·n(CH_3NO_2).illustrating the capping of a bowl-in-bowl pair (in green) by three type B [{$Re(CO)_3Br$}$_3$(L1)] complexes.

The crystal structure of the complex [{$Re(CO)_3Br$}$_3$(L3)]·n(DMSO) (= **3**·n(DMSO)) was solved in the chiral hexagonal space group *P*321. The asymmetric unit comprises one third of the [{$Re(CO)_3Br$}$_3$(L3)] which is sited around a 3-fold rotation axis and fragments of a highly disordered DMSO molecule site on the 3-fold axis. As expected, each 2,2':6',2''-terpyridine ligand moiety of L3 binds to a Re(I) cation through only two adjacent pyridyl groups, with the third pyridyl unbound and rotated at a torsion angle of -124.6°, Figure 4a. The Re(I) cation has a distorted octahedral environment with a fac arrangement of CO ligands and a Br^- ligand cis to the two chelating pyridyl groups, and the {$Re(CO)_3Br$(terpy)} fragment is structurally similar to mononuclear analogues.[26] Unlike for complex **1**·n(CH_3NO_2) the molecular cavity of the cavitand ligand is occupied by a small guest molecule with a highly disordered DMSO guest occupying the cavity, Figure 4a. The Br^- ligands are oriented away from the molecular bowl. In the crystal lattice aligned columns of [{$Re(CO)_3Br$}$_3$(L3)] complexes separated by the guest DMSO are formed, at a separation equivalent to the *c* unit cell length of 9.5684(5) Å. Adjacent columns in

the crystal lattice have opposite orientations of the cavitand bowls and the {$Re(CO)_3Br$(terpyridyl-benzyl)} arms intercalate between the columns, shown for one such motif in Figure 4b.

The overall crystal lattice is shown in Figure 4c. The intercalating columns of [{$Re(CO)_3Br$}$_3$(L3)] complexes forms an array with large propeller-shaped channels running down the *c* crystallographic unit cell. The un-coordinated pyridyl groups of L3 and some carbonyl ligands are oriented into these channels. The channels are likely to be filled with additional DMSO as the channels account for approximately 50% of the unit cell volume, however these could not be reliably located in the crystal structure. An interesting feature of the structure of **3**·n(DMSO) is that all L3 ligand enantiomers within the structure are of the same chirality. Hence the material is a conglomerate, forming a racemic mixture of chirally pure single crystals from an enantiomeric mixture of isomers in solution. Conglomerate formation has also been reported for a small number of other CTG-type systems.[28a,29]

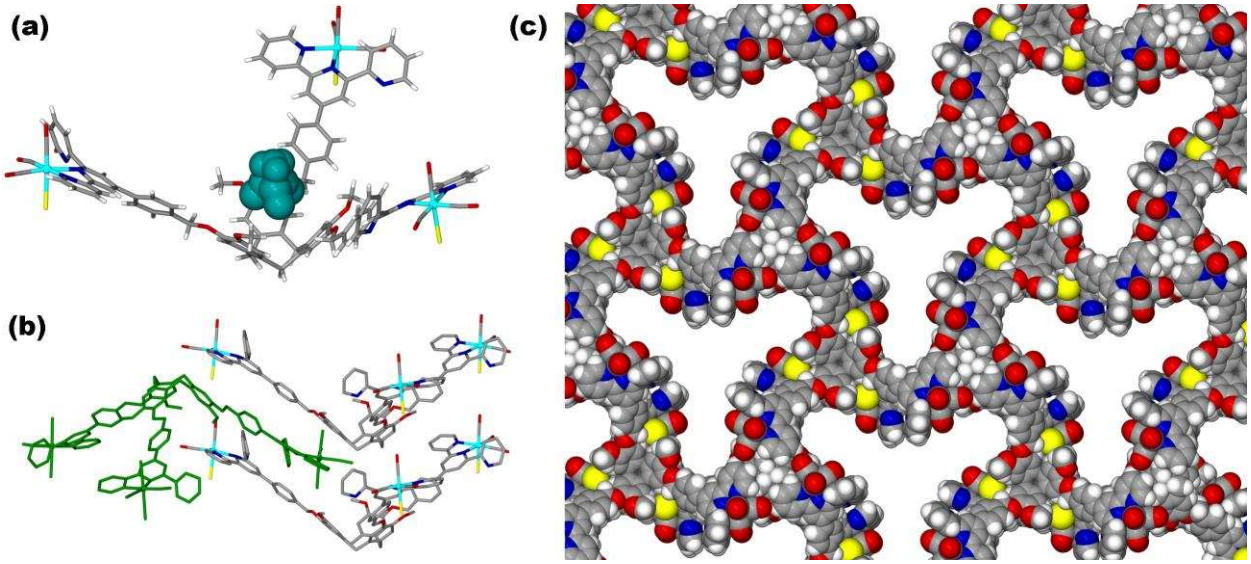

Figure 4. Crystal structure of complex [{$Re(CO)_3Br$}$_3$(L3)]·n(DMSO) (= **3**·n(DMSO)). (a) [{$Re(CO)_3Br$}$_3$(L3)] complex with disordered guest DMSO (large spheres); (b) stacking of identically oriented [{$Re(CO)_3Br$}$_3$(L3)] complexes, and intercalation of complex with opposite orientation (in green); (c) space-filling view of channels formed down *c* axis.

Photophysical Properties

Absorption and luminescence properties of ligands and complexes were determined in DMSO solution and summarised in Table 1. Rhenium tricarbonyl complexes of bipyridines and related ligands emit from triplet states following excitation which usually has a large degree of metal-to-ligand charge transfer (MLCT) involving relocation of an electron from the t_{2g}^6 Re(I) centre to the vacant bipyridine π* orbitals. Halido- complexes of the general formula [$Re(CO)_3$(bpy)Br/Cl] often offer low energy excitation and emission due to an additional character of ligand-to-ligand charge transfer, specifically from the halide lone pair to the bipyridine π*.[11] As rapid inter-system-crossing mediated by spin-orbit coupling allows efficient population of the triplet excited states (^{3}MLCT) such complexes often offer the attractive long lifetimes and large Stokes shifts characteristic of forbidden transitions. The electronic (uv-vis) spectrum of complex **1** (Figure 5a) shows a series of overlapping absorptions with maxima around 290 and 320 nm, typical of intraligand transitions and additionally a broad shoulder to the lower energy edge of these transitions with a maximum around 365 nm but extending well into the visible region with significant absorption at 460 nm. This low energy shoulder is typical of, and tentatively assigned to, a transition with ^{1}MLCT Re(*d*)-bpy π* nature with intraligand (IL) contributions as discussed above. The nature of this absorption band was confirmed by steady state luminescence spectroscopy when excitation at 385 nm led to strong visible emission.

Emission and excitation spectra were recorded at room temperature and revealed that complex **1** demonstrates a relatively long maximum excitation wavelength, centred at 450 nm, which is significantly longer than many of the previously examined mononuclear rhenium complexes, although not exceptionally so for the halido- species, and matches the lower energy end of the electronic absorption band assigned as ^{1}MLCT.[30] Complex **1** shows an emission maximum at 590 nm, giving a Stokes shift of ~ 150 nm, with such large values being typical of ^{3}MLCT emission (see Figure 5b and Table 1).

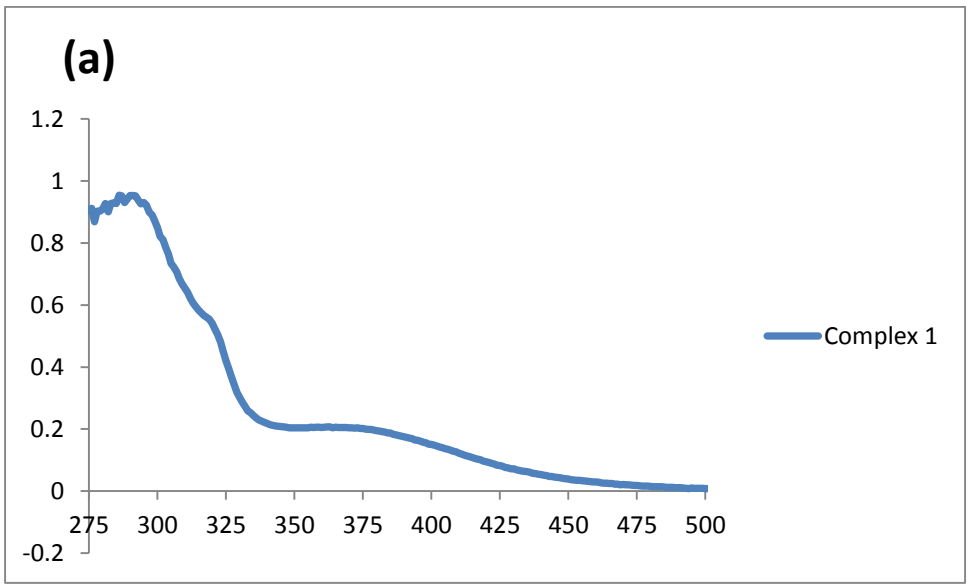

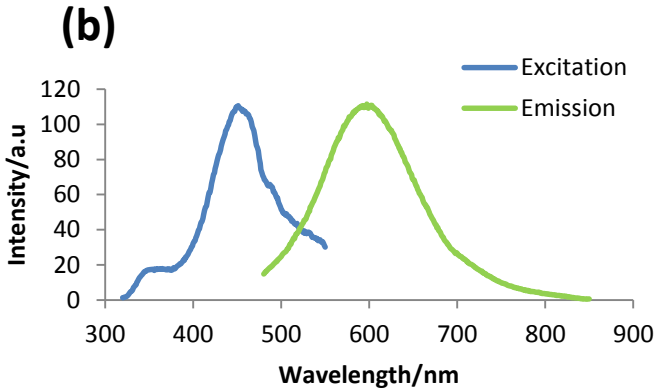

Figure 5: Photophysical behaviour of complex **1.** (a) Electronic absorption spectrum of complex **1** DMSO**.** (b) Excitation and Emission spectra of complex [{$Re(CO)_3Br$}$_3$(L1)] **1** in DMSO solution, showing red-shifted emission (emission spectrum excited at 450 nm, excitation spectrum recorded with emission monochromated at 600 nm).

The electronic spectrum of complex **2** (Figure 6a) shows a series of high energy absorptions around 275-350 nm typical of intraligand transitions, and additionally two broad shoulders to the lower energy edge of these transitions, the first centred around 330 nm, and the second with a maximum around 380 nm but extending well into the visible region with significant absorption beyond to 450 nm. This lowest energy shoulder is again assigned to a ^{1}MLCT absorption as before, but the 380 nm band represents a transition unobserved in complex **1**. In the luminescence spectra complex **2** shows unusual behaviour, exhibiting two excitation maxima at 365 and 462 nm, and two emission maxima at approximately 530 and 650 nm (see Figure 6b). The lowest energy emission peak at 650 nm is over 50 nm longer wavelength than that of the ether analogue complex **1** which can be attributed to the greater stabilisation of the π^* orbitals of complex **2** by increased conjugation lowering the HOMO-LUMO energy gap. The observation of dual excitation and emission bands in complex **2** led to a closer examination of the photophysical properties of this complex. Dual emission from metal complexes is by no means unknown,[31] but is still a relatively rare phenomenon, and it is important to prove that the apparent peaks are emission from different electronic states of the complex, rather than Raman bands, or similar artefacts. In this case the bands were clearly of different electronic origin, with their positions not varying as a result of excitation wavelength (thus eliminating Raman effects) but with the relative intensities of the two bands altering as a function of excitation wavelength.

As can be seen in Figure 6c, in fact, exciting the higher energy excitation band biases emission towards the lower energy emission band, and vice versa, demonstrating that these must be separate electronic processes. As it is not clear how the portion of the complex containing the rhenium bipyridine unit could host two such different excited states, and as the emission band at c. 530 nm appears not to be as broad as a typical MLCT band, an examination of the photophysical properties of the ligands was undertaken. Both L1 and L2 have two bands in the emission spectrum, (L1 at 405 and 450 nm, L2 at 420 and 470 nm, supporting information Figs S26, S27) and in both cases the bands can be preferentially excited by irradiating at different parts of the spectrum (see Table 1). However, in both cases the lower energy excitation excites the lower energy emission, and each band is red-shifted in L2 by 10-15 nm which indicate similar processes operate in each ligand and these bands are tentatively assigned to mixed $n/\pi-\pi^*$ transitions associated with the veratrole-, (higher energy)[32] and bipyridine- (lower energy)[33] derived portions of the chromophores. L3 shows an emission band with a slight shoulder at ca. 425 nm with a max excitation wavelength of 355 nm (see table 1 and supporting information Fig. S28). Again these bands are tentatively assigned to mixed $n/\pi-\pi^*$ transitions.

(a)

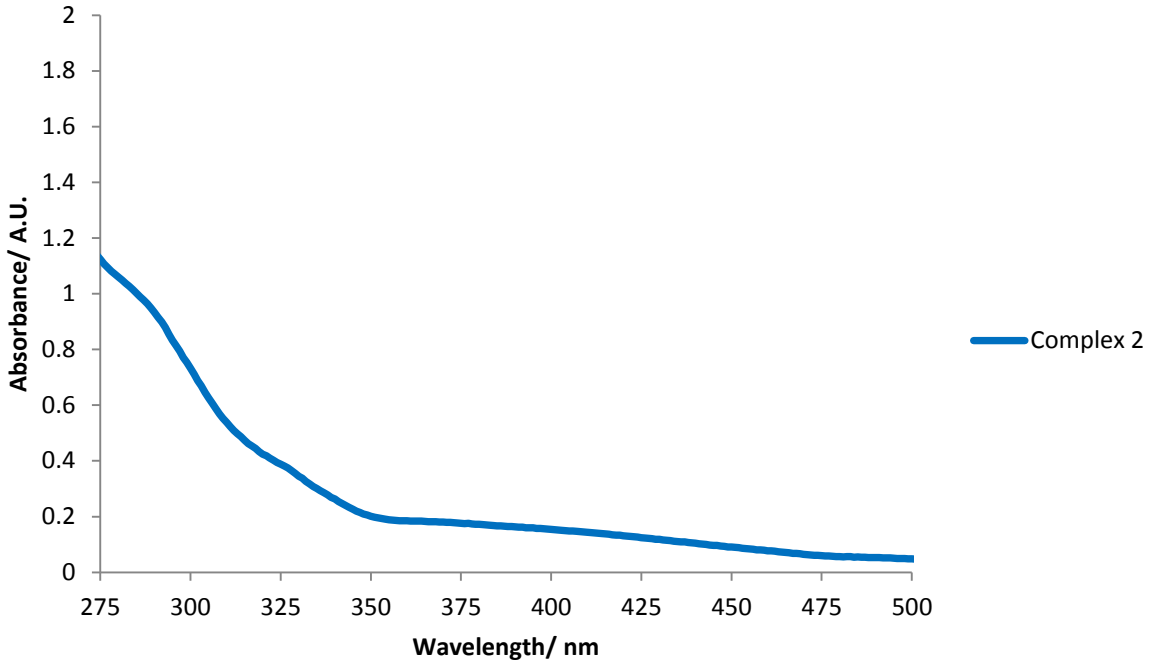
Absorbance/ A.U.
2
1.8
1.6
1.4
1.2
1
0.8
0.6
0.4
0.2
0
275
300
325
350
375
400
425
450
475
500
Wavelength/ nm
Complex 2

(b)

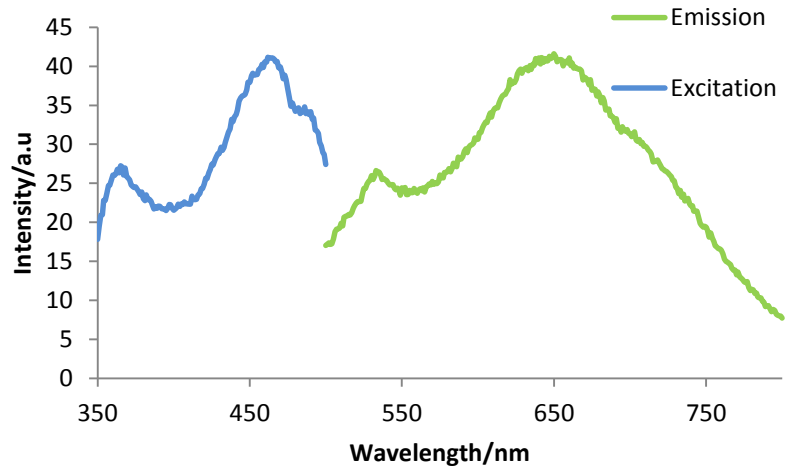
Intensity/a.u
45
40
35
30
25
20
15
10
5
0
350
450
550
650
750
Wavelength/nm
Emission
Excitation

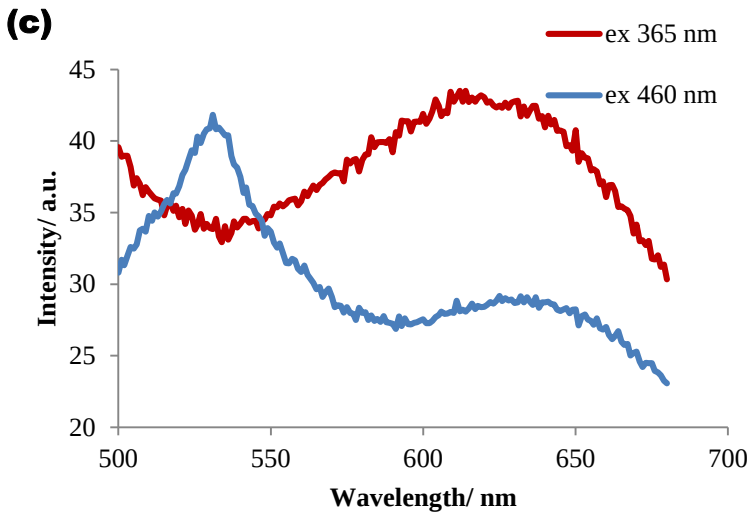

Figure 6: Photophysical behaviour of complex [{$Re(CO)_3Br$}$_3$(L2)] **2**. (a) Electronic absorption spectrum in DMSO. (b) Steady-state Excitation and Emission spectra; (c) Emission spectra recorded at varying excitation wavelength.

As the nature of the anomalous emission in complex **2** remained unclear, time-resolved studies were undertaken using pulsed laser and TCSPC methods, in order to further probe the electronic natures of the transitions involved (supporting information Figs. S29-S31). Both L1 and L2 showed lifetimes typical of simple organic systems (4-6 ns) with no significant variation between the lifetimes recorded for the various peaks. L3 exhibits an even shorter lifetime best described by two 1-2 ns components, again typical of organic systems (Figure S28, supporting information). Complex **1** had a long lifetime of 459 ns, which is in the region expected for ^{3}MLCT emission, and the decay fitted well to a single component, suggesting that the emission occurs from a single electronic state. However, complex **2** showed decay profiles which differed depending upon the wavelength of monochromation of the detection, and could not be fitted to a single component decay. The best meaningful fit was obtained by modelling a two component decay with lifetimes of 3 and 21 ns, which gave an acceptable χ^2 value of 0.989. TRES

(supporting information) suggested that in fact the two components in the decay arise from two different emission maxima, approximating to the two emission maxima seen in the steady state spectrum (but with a bias to longer wavelengths attributed to tailing). The shorter wavelength, shorter lifetime band would appear to be of singlet ligand based nature. Although the 50 nm difference between the emission of free ligand **2** (470 nm) and the anomalously sharp emission peak observed in complex **2** is too large to be explained by the generation of free ligand upon irradiation, a series of spectra were recorded before and after fluorescence experiments (see Figure S32 Supporting information). As it would usually be expected that excitation of the bipyridine portion of the complex would lead to ^{3}MLCT emission, it is likely that this residual ligand fluorescence is associated with the veratrole unit, with the bands red-shifted due to the electronic effects of complexation being communicated through the ester linkage.

On the basis of all these data, considering the peak shapes, positions and lifetime profiles, it is therefore tentatively suggested that the anomalously sharp band in the emission spectrum of complex **2** at 530 nm which is associated with a lifetime of around 3 ns is of ligand-based, singlet origin, and represents a veratrole-centred transition analogous to the peak in ligand **2** observed at 470 nm which has undergone a 50 nm red-shift upon coordination, but is not undergoing intersystem crossing to the triplet, and is best considered as purely ligand based. The broader peak at around 650 nm, associated with a longer lifetime is proposed to be of triplet MLCT origin, with its shorter luminescence lifetime in comparison with complex **1** being predicted by energy gap law, whereby the red shifted emission indicates a smaller energy gap, and therefore a greater rate of non-radiative deactivation, which also acts as a quenching mechanism and weakens the emission associated with complex **2**.[11b]

The electronic (uv-vis) spectrum of complex **3** shows a series of overlapping absorptions peaking around 280 with shoulders around 310 and 330 nm, typical of intraligand transitions (see Figure 7a). These bands are broader and less well defined than for complexes **1** and **2** which is consistent with the expected fluxional nature of the coordination environment in which the electronic transitions take place rapidly on the exchange timescale leading to overlap of signals derived from many micro-environments. There is also a broad shoulder to the lower energy edge of these transitions with a maximum around 360 nm but extending well into the visible region with significant absorption at 430 nm. As for the other complexes, this low energy shoulder is assigned to a transition with ^{1}MLCT Re(*d*)-bpy π^* nature with IL contributions as discussed above.

Investigation of this band by luminescence spectroscopy exciting at 350 nm led to visible emission centred at 460 nm, Figure 7b. The excitation spectrum with emission monochromated at 460 nm showed a series of low energy excitation maxima at 365, 395 and 415 nm. Interestingly, excitation at different wavelengths within this region led to the maximum emission wavelength changing with excitation from 350 to 450 nm giving emission maxima from 460 to 510 nm, with intensity dropping at excitation wavelengths longer than 420 nm, Figure 7c. Comparison of the excitation spectra with emission monochromated at 460 and 510 nm respectively, Figure 7d, showed that the three maxima observed in the original (emission 460 nm) spectrum are also observed in the spectrum monochromated at 510 nm, however with the relative intensities reversed. This is interpreted as the emission spectrum consisting of a series of broad overlapping bands arising from different electronic origins, each of these being excited through irradiation of the broad bands observed in the excitation spectra. Dual emission (see above) and excitation-dependent emission wavelengths are in breach of one of the principles of

photophysics, Kasha's rule,[34] which states that emission from any molecule should be seen from only the lowest energy band of a given multiplicity (i.e. single invariable wavelengths). Rather than implying that complex **3** emits from multiple excited states in true breach of Kasha's rule, it is likely that the observed phenomena arise from what are effectively different molecular species. Complex **3** contains three rhenium centres, each of which is coordinated by two of the three possible nitrogens of a terpyridine ligand. In solution rapid exchange between the coordinated and free terminal pyridines is observed and therefore each rhenium has at least two coordination environments, regardless of the mechanism of fluxionality.[26] Given the relative rates of electronic transitions compared to the exchange mechanisms these should be considered as separate species, and given that there are three rhenium centres per complex, each with at least two possible environments, there are at least eight solution species absorbing and emitting light. Thus, the excitation-dependent emission is likely to result from multiple different coordination isomers absorbing and emitting at different wavelengths but so close together and that the emission spectrum appears as a continuum.

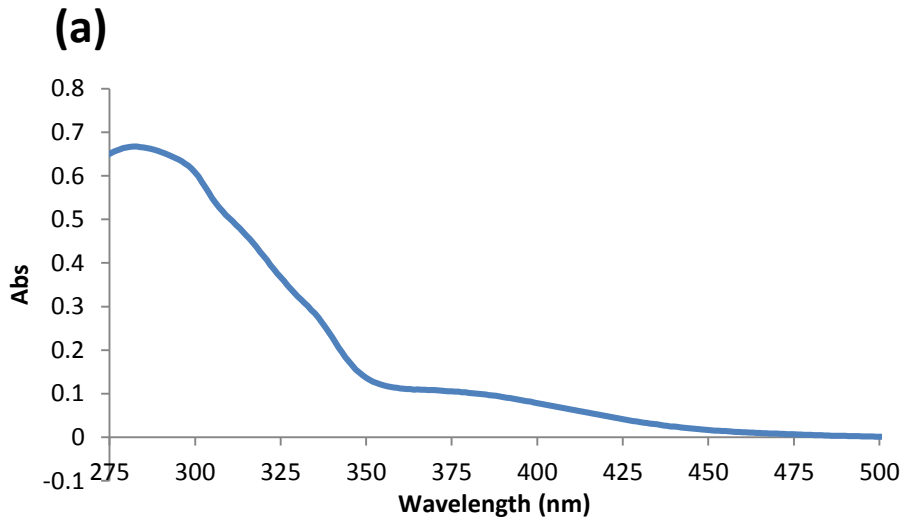

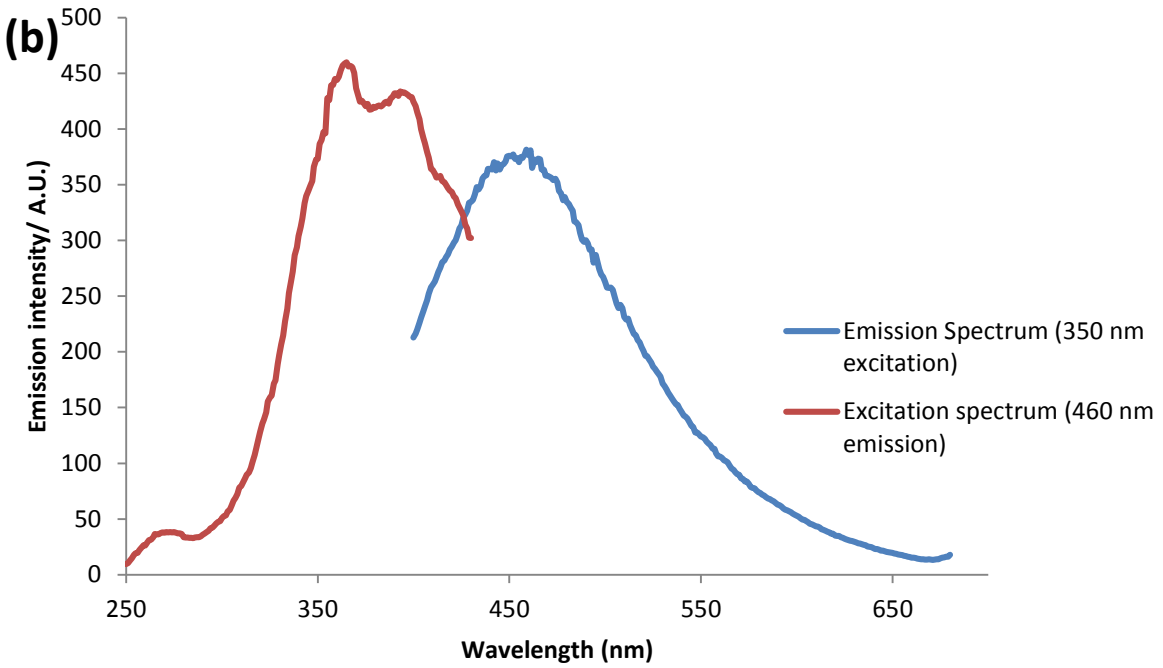
(b)
Emission intensity/ A.U.)
500
450
400
350
300
250
200
150
100
50
0
250
350
450
550
650
Wavelength (nm)
Emission Spectrum (350 nm excitation)
Excitation spectrum (460 nm emission)

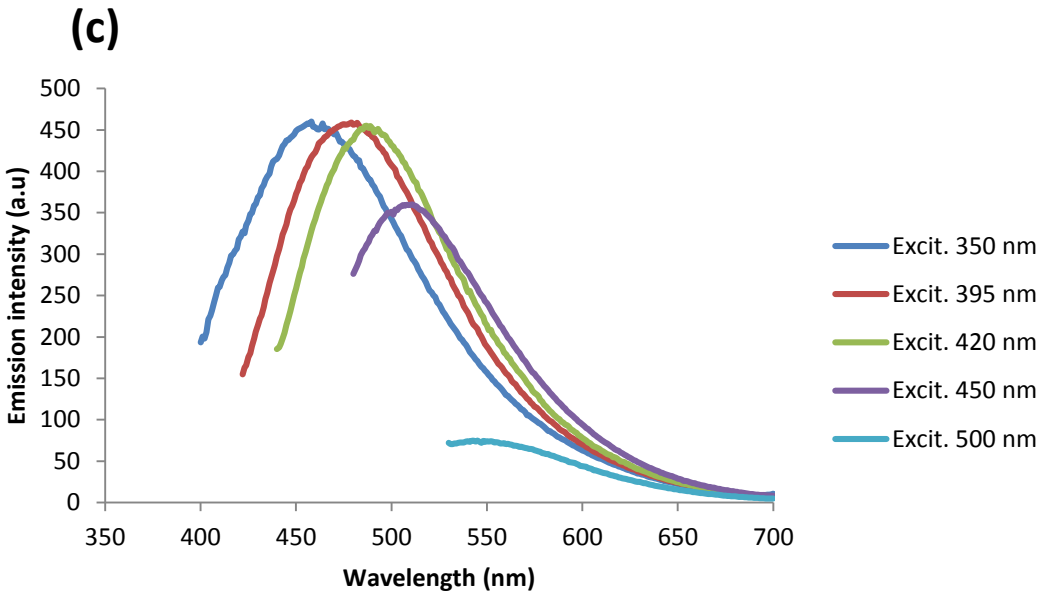
(c)
Emission intensity (a.u)
500
450
400
350
300
250
200
150
100
50
0
350
400
450
500
550
600
650
700
Wavelength (nm)
Excit. 350 nm
Excit. 395 nm
Excit. 420 nm
Excit. 450 nm
Excit. 500 nm

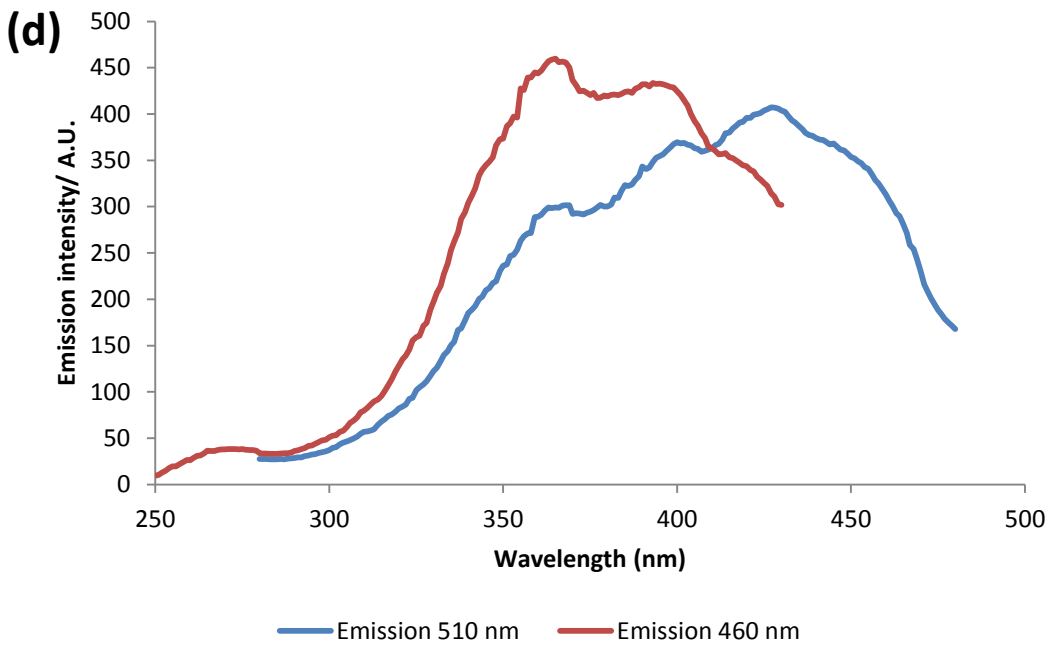

Figure 7: Photophysical behaviour of complex [{$Re(CO)_3Br$}$_3$(L3)] **3**. (a) Electronic absorption spectrum in DMSO (b) Steady State Emission and Excitation Spectra. (c) Variation of emission profile with excitation wavelength. (d) Excitation spectra with emission monochromated at 460 and 510 nm.

Time-resolved fluorescence spectroscopy revealed complex **3** to have much shorter lifetime decays than the bands assigned to MLCT emission in complexes **1** and **2**, and that the decays were multicomponent. It should be noted that the short lifetime component of complex **2** is assigned as singlet in nature and thus cannot be compared to the MLCT- assigned bands.The best fit for a decay collected at 460 nm (excitation 375 nm) was to three components of 1, 3 and 11 ns of fractional intensities 22, 48 and 30 % respectively, but it is likely that there are more than three components to the decay and it would be unwise to interpret these data further than as

reinforcing the multicomponent nature of emission from this complex. The much shorter lifetimes / average lifetime of emission from complex **3** are understandable in terms of both the fluxional nature of the system providing multiple opportunities for vibrational losses in a system which has a large number of geometries and arrangements, and also in terms of the large number of energy and electron transfer possibilities. In a system in which there are at least 8 different possibilities for the coordination environment at rhenium per complex it is highly likely that upon photoexcitation the initially formed excited state can access a lower energy analogue by intramolecular energy / electron transfer. If the different isomeric geometries are close in energy then thermal back-transfer may also occur, allowing rapid multiple exchanges and shortening overall lifetimes. Although the behaviour may be explicable in terms of coordination isomerism, nevertheless any report of a new complex which breaches Kasha's rule is noteworthy.

Table 1: Summary of photophysical data

Entry	**λ max em (nm)**	**λ max ex (nm)**	**τ (ns)**	**Assignment**
L1	410	340	5	IL veratrole
L1	450	360	6	IL bipyridine
L2	420	345	4	IL veratrole
L2	470	390	5	IL bipyridine
L3	425	355	1	IL veratrole
complex **1**	590	450	459	MLCT
complex **2**	530	460	3	IL?
complex **2**	650	365	21	MLCT

complex **3**	450-500 nm	350-420 nm	1, 3,11	MLCT

Conclusions

In conclusion we have synthesized a novel bypridine-functionalised ligand and three novel $Re(CO)_3Br$-cavitand complexes which show interesting red-shifted luminescent properties and long wavelength excitation maxima which differ dependent on the nature of the linkage of the bipyridine donors to the CTG scaffold (ester vs. ether).

The c. 500 ns lifetime of complex **1** is ideal for biomedical cell imaging, as time-gated collection can be employed; where a pulse of light is used to excite the complex after it has been taken up into cells, a fixed time is allowed to pass, and then the emission spectrum is recorded. This technique allows any short-lived auto-fluorescence from surrounding tissue to occur and yet not be recorded in the final emission profile, thereby eliminating any uninformative fluorescence data from endogenous species such as NADP and flavones. Meanwhile, dual emission from complex **2**, in addition to the academic interest in complex photophysics, offers possibilities of ratiometric sensing of analytes which would preferentially quench one of the components, e.g. specific quenching of ^{3}MLCT by $^3O_2$.[35]

The introduction of carboxylic acid groups onto the bipyridine donors arms are thought to cause shorter-lived lifetimes of the excited-state rhenium complexes in aqueous solution,[36] but reasonably long lifetimes can still be recorded in acetonitrile solution. The closest analogous complex reported to the Re-halo complexes in this manuscript, [Re(4-Me,4'-CO_2H-bipyridyl)$(CO)_3$Cl] showed a lifetime of <25 ns in aqueous solution (regardless of pH), while in acetonitrile the lifetime extended to 60-70 ns depending upon conditions. A direct comparison

with the lifetime of the carbonyl-substituted complex **2** is complicated by the dual emission observed with this species, but even the longer component (21 ns) is shorter that that recorded for [Re(4-Me,4'-CO_2H-bipyridyl)$(CO)_3$Cl] in acetonitrile. However, given that this emission band in complex **2** is red shifted by 50 nm compared to [Re(4-Me,4'-CO_2H-bipyridyl)$(CO)_3$Cl] (650 nm vs 601 nm[36]) it is likely that energy gap law[11b] plays a larger role in this lifetime reduction than solvation effects. Linking the carboxyl groups to a donor/acceptor group allows a photoinduced electron transfer route to be accessed for the complex meaning that $Re(CO)_3(CH_3$bipyCOOR)X species may have potential as photosensitizers in electron transfer reactions.[36] These complexes, when linked through amides rather than esters, are also capable of acting as sensitizers for near-infrared lanthanide luminescence with Nd^{III}, Eu^{III} and Yb^{III}.[37]

The possibility to further modify the complexes through abstraction of the halides and coordination of another heteroatom donor could give them potential to be tailored as photoactive materials with tunable emission properties, as luminescent sensors or biological targeting agents, but also as large functional tectons for the formation of large, complex metallo-supramolecular architectures.

Experimental

Synthesis

(±)-Cyclotriguaiacylene,[38] (±)-tris(4-[4-methyl-2,2'-bipyridyl]methyl)cyclotriguaiacylene (L1) [25] and (±)-tris(4-[2,2',6',2''-terpyridyl]benzyl)cyclotriguaiacylene (L3) [7] were synthesized according to literature methods. All other chemicals were obtained from commercial sources and were used without further purification. NMR spectra were recorded by automated procedures on a Bruker DPX 300 MHz NMR spectrometer. Electrospray mass spectra (ES-MS) were measured on a Bruker Maxis Impact instrument in positive ion mode. Infra-red spectra were recorded as solid

phase samples on a Bruker ALPHA Platinum ATR. Elemental analyses were performed on material that had been washed with diethyl ether, subsequently dried at 80-90 ˚C under vacuum and then exposed to the atmosphere.

(±)-2,7,12-Trimethoxy-3, 8, 13-tris(4-(4'-methyl-2, 2'-bipyridoyl))-10, 15-dihydro-5H-tribenzo[a, d, g]cyclononene (tris(4-[4'-methyl-2,2'-bipyridoyl])cyclotriguaiacylene) (L2) Cyclotriguaiacylene (0.369 g, 0.97 mmol) was dissolved in anhydrous tetrahydrofuran (60 mL) under a nitrogen atmosphere and cooled to -78°C. Triethylamine (2 mL) was added to the solution and stirred for 1 hour at -78°C. 4'-Methyl-2,2'-bipyridine-4-carbonyl chloride (0.800 g, 0.76 mmol) was added to the reaction flask and the solution stirred for a further 2 hours at -78°C, then allowed to come to room temperature and stirred for a further 3 days. The solvent was then removed in vacuo to give a pale off-pink solid that was triturated with EtOH to give the title compound as an off-white solid (0.655 g, 0.687 mmol, 76%); ^{1}H NMR (300 MHz, DMSO-d6) δ (ppm) 9.02 (s, 1H, H^{6}), 9.00 (s, 1H, $H^{6'}$), 8.64 (d, J = 4.8 Hz, 1H, H^{5}), 8.35 (s, 1H, H^{3}), 8.03 (d, J = 5.4 Hz, 1H, $H^{5'}$), 7.68 (s, 1H, aryl CTG), 7.41 (s, 1H, aryl CTG), 7.39 (s, 1H, $H^{3'}$), 4.96 (d, J = 13.8 Hz, 1H, HC<u>H</u> endo), 3.79 (m, J = 9.1 Hz, 4H. <u>H</u>CH exo/OMe), 2.49 (s, 3H, Me); ^{13}C NMR (75 MHz, $CDCl_3$) δ (ppm) 163.40, 157.64, 155.09, 149.95, 149.20, 148.28, 138.33, 137.93, 131.45, 125.17, 123.92, 123.25, 122.13, 121.14, 114.26, 109.98, 77.43, 77.24, 77.01, 76.59, 56.26, 21.20; TOF-MS ESI: m/z = 997.3569 (M^{+}); Analysis for $C_{60}H_{48}N_6O_9.(2(H_2O)$ (% calculated, found) C (69.76, 69.90) H (5.07, 4.75) N (8.13, 7.80); Infrared analysis IR (solid state): ν_{max} = 1757 (OCO), 1610, 1594, 1557, 1458, 1443, 1400, 1278, 1233, 1139, 1090, 1065, 991, 919, 836, 768, 751.

[(Re(Br)(CO)$_3$)$_3$(tris(4-[4'-methyl-2,2'-bipyridyl]methyl)cyclotriguaiacylene)] complex 1

$Re(CO)_5Br$ (67.9 mg, 0.167 mmol) was added to L1 (50 mg, 0.05 mmol) in toluene (15 mL) and heated to reflux for 24 hours to form an orange solution and bright yellow precipitate. The precipitate was removed through sinter filtration, and washed with cold toluene (15 mL) and diethyl ether (10mL) to give a crystalline yellow solid (101 mg, 96 %); ^{1}H NMR (300 MHz, Acetonitrile-d_3) δ (ppm) 8.96 (d, J = 6.2 Hz, 1H, $H^{6'}$), 8.88 – 8.72 (m, 1H, H^6), 8.42 (d, J = 5.7 Hz, 1H, $H^{3'}$), 8.21 (d, J = 12.2 Hz, 1H, H^3), 7.61 (s, 1H, $H^{5'}$), 7.43 (s, 1H, H^5), 7.12 (s, 1H, aryl CTV), 7.02 (s, 1H, aryl CTV), 5.26 (s, 2H, OC$\underline{H}_2$), 4.73 (d, J = 13.8 Hz, 1H, $\underline{H}$CH), 3.79 (d, J = 8.6 Hz, 3H, OMe), 3.56 (d, J = 13.7 Hz, 1H, HC$\underline{H}$), 2.53 (d, J = 5.5 Hz, 3H, Me); ^{13}C NMR (75 MHz, DMSO) δ (ppm) 197.35, 189.53, 155.25, 154.59, 153.03, 152.43, 152.24, 151.51, 145.80, 133.80, 132.00, 128.48, 125.19, 124.85, 114.32, 109.50, 68.95, 56.00, 35.08, 20.89; TOF-MS ESI: m/z = 1925.0643 $[(Re_3(CO)_9(Br)_2)L1]^+$ (1925.0638); Analysis for $C_{69}H_{54}Br_3N_6O_{15}\cdot 2(H_2O)$ (% calculated, found) C (40.59, 40.40) H (2.86, 2.80) N (4.12, 4.10); IR (solid state): ν_{max} = 2017.14, 1883.24 (C≡O), 1180.14 (C-O), 1616, 1505, 1487, 1416, 1273, 1180, 1088, 1031, 973, 888, 826, 646.

[(Re(Br)(CO)$_3$)$_3$(tris(4-[4'-methyl-2,2'-bipyridoyl])cyclotriguaiacylene)] complex 2

$Re(CO)_5Br$ (0.131g, 0.321 mmol) was added to L2 (0.100 g, 0.100 mmol) in toluene (15 mL) and heated to reflux for 24 hours to form an orange solution and bright yellow precipitate. The precipitate was removed through sinter filtration, and washed with cold toluene (15 mL) and diethyl ether (10mL) to give a crystalline yellow solid (193 mg, 94%); ^{1}H NMR (300 MHz, DMSO-d6) δ (ppm) 9.30 (d, J = 6.0 Hz, 1H, H^6), 9.21 (s, 1H, H^3), 8.97 (s, 1H, $H^{3'}$), 8.90 (d, J = 5.7 Hz, 1H, H^6), 8.26 (d, J = 5.6 Hz, 1H, H^5), 7.66 (s, 1H, CTG aryl), 7.63 (d, J = 5.2 Hz, 1H, $H^{5'}$), 7.37 (s, 1H, CTG aryl), 4.97 (d, J = 13.9 Hz, 1H, HC$\underline{H}$ endo), 3.76 (s, 4H, OMe/$\underline{H}$CH exo),

2.58 (s, 3H, Me); ^{13}C NMR (75 MHz, DMSO) δ (ppm) 197.01, 189.09, 161.42, 157.10, 154.54, 153.90, 152.62, 152.43, 148.99, 139.17, 138.94, 137.42, 131.98, 128.92, 126.61, 126.01, 123.29, 114.51, 109.48, 56.27, 35.05, 20.72; TOF-MS ESI: m/z = 2045.0152 (M – Br + DMSO); Analysis for $C_{69}H_{48}Br_3N_6O_{18}$ (% calculated, found) C (40.48, 40.20) H (2.36, 2.60) N (4.10, 4.10); IR (solid state): ν_{max} = 2020 (C≡O), 1889 (2 x C≡O), 1748 (OCO) 1618, 1505, 1409, 1324, 1302, 1251, 1232, 1205, 1176, 1140, 1101, 1070, 991, 895, 833, 767, 645.

[(Re(Br)(CO)$_3$)$_3$(tris-(4-[2,2',6',2"-terpyridyl]benzyl)cyclotriguaiacylene)] complex 3

$Re(CO)_5Br$ (0.131g, 0.321 mmol) was added to L3 (0.100 g, 0.100 mmol) in toluene (3 mL) and heated to 110 °C for 24 hours to form an orange suspension in a colorless solution. The product was collected by filtration to give a yellow precipitate which was washed with diethyl ether (10mL) to give a crystalline yellow solid (168 mg, 95%); ^{1}H NMR δ_H (300 MHz, DMSO) δ (ppm) 9.04 (s, 9H, H^6, $H^{3'}$, $H^{5'}$), 8.77 (s, 3H, $H^{6''}$), 8.40 – 8.23 (m, 3H, H^5), 8.21 – 8.08 (m, 9H, H^3, Ph), 8.02 (ps. t, J = 7.8 Hz, 3H, $H^{4''}$), 7.90 – 7.78 (m, 3H, $H^{3''}$), 7.79 – 7.66 (m, 3H, H^4), 7.67 – 7.48 (m, 9H, $H^{5''}$, Ph), 7.17 (s, 3H, Aryl CTG), 7.01 (s, 3H, Aryl CTG), 5.18 (s, 6H, CH_2), 4.69 (d, J = 13.5 Hz, 3H, endo C<u>H</u>H), 3.65 (s, 9H, Me), 3.48 (d, J = 13.5 Hz, 3H, exo CH<u>H</u>). δ_C (75 MHz, DMSO) 197.13, 195.74, 190.06, 157.62, 156.91, 156.01, 152.46, 148.92, 147.40, 145.77, 140.26, 139.52, 136.62, 133.54, 131.69, 127.75, 127.55, 127.12, 125.09, 124.64, 123.93, 120.21, 55.80, 40.07, 39.80, 39.52, 39.24, 38.96, 38.69, 38.41, 36.37. Analysis for $C_{99}H_{69}Br_3N_9O_{15}Re_3.3(H_2O)$ (% calculated, found) C (48.00, 47.80) H (3.05, 2.95) N (5.09, 4.70); IR (solid state): ν_{max} = 2018 (C≡O), 1886 (2 x C≡O), 1608, 1568, 1507, 1486, 1427, 1396, 1262, 1216, 1186, 1144, 1086, 1013, 992, 908, 848, 827, 785, 745, 645.

Photophysical Studies

UV vis spectra were recorded on an Agilent Technologies Cary 60. Steady state emission and excitation spectra were recorded on an Agilent Technologies Cary Eclipse on optically dilute samples (absorbance of 0.1 at excitation wavelength) except in the case of the variable excitation wavelength series of complex **3** which were run at constant concentration (A = 0.1 at 350 nm) with slit widths of 10 nm for both excitation and emission monochromators. Time-resolved spectra were recorded on a PicoQuant FluoTime 300 exciting with an LDH-P-C-375 and decays analysed with the program FluoFit. Photophysical studies were performed in DMSO (to ensure full dissolution of the solids). The lifetime of the complex is defined as the time at which the emission intensity has dropped to e^{-1} times the initial intensity I_0. To calculate this value the dark counts must be taken into account, as the intensity of the emission does not drop to 0, but plateaus at ~2000 a.u. The data must be normalised to reflect the baseline dark count. Therefore the average dark count value is subtracted from all recorded intensities to give an I_0 of 8000 a.u. As stated, $I_\tau = I_0 \times e^{-1}$, leading to an I_τ value of 2943 a.u., which corresponds to a τ value of 0.467 μs, or 467 ns for complex **1** and a two component lifetime of 3 ns and 23 ns for complex **2** as confirmed by TRES measurements and analysis with FluoroFit.

X-ray Crystallography

Crystals were mounted under inert oil on a MiTeGen tip and flash frozen to 100(1) K using an OxfordCryosystems low temperature device. X-ray diffraction data were collected using Cu-Kα radiation (λ= 1.54184 Å) using an Agilent Supernova dual-source diffractometer with Atlas S2 CCD detector and fine-focus sealed tube generator. Data were corrected for Lorenztian and polarization effects and absorption corrections were applied using multi-scan methods. The structures were solved by direct methods using SHELXS-97 and refined by full-matrix on F^2 using SHELXL-97.[39] Unless otherwise specified, all non-hydrogen atoms were refined as

anisotropic, and hydrogen positions were included at geometrically estimated positions. Crystals of L1·(Et_2O) were of poor quality, with poor internal consistency (R_{int} = 0.1955) and only exhibited weak diffraction, with no diffraction at high angles. Attempts to grow higher quality crystals were not successful. For complex **1**·n(CH_3NO_2) solvent CH_3NO_2 and some CO ligands were refined isotropically and one C=O bond length restrained. For complex **3**·n(DMSO) carbonyl ligands and disordered DMSO were refined isotropically, and restraints were placed on some C=O and metal-carbonyl bond lengths. Hydrogen positions were not calculated for the highly disordered DMSO. Both **1**·n(CH_3NO_2) and **3**·n(DMSO) contained significant void space with residual electron density which could not be meaningfully modelled as solvent, hence the SQUEEZE routine of PLATON was employed in these structures.[40] Additional details of data collections and structure solutions are given in Table 2, given formulas correspond to the levels of solvation shown by crystallography.

Table 2. Details of data collections and structure refinements.

Compound	L1·(Et_2O)	**1**·n(CH_3NO_2)	**3**·n(DMSO)
Formula	$C_{64}H_{64}N_6O_7$	$C_{141}H_{117}Br_6N_{15}O_{36}Re_6$	$C_{101}H_{74}Br_3N_9O_{16}Re_3S$
Mr	1029.21	4194.16	2500.08
Crystal color and shape	Colorless, plate	Yellow, polyhedral	Yellow, needle
Crystal size (mm)	0.20 x 0.10 x 0.01	0.10 x 0.10 x 0.20	0.40 x 0.03 x 0.03
Crystal system	Orthorhombic	Trigonal (hexagonal axes)	Hexagonal
Space group	Pbna	R-3	P321
a (Å)	9.308(2)	29.1454(12)	31.4303(16)
b (Å)	34.568(10)	29.1454(12)	31.4303(16)
c (Å)	33.811(9)	42.570(3)	9.5684(5)
α (^{0})	90	90	90
β (^{0})	90	90	90
γ (^{0})	90	120	120
V (Å^3)	10879(5)	31317(3)	8185.9(7)
Z	8	6	2
ρ_{calc} (g.cm^{-3})	1.257	1.334	1.014

θ range (^{0})	4.68 – 45.0	3.65-58.99	3.25-73.03
No. data collected	23412	16678	18704
No. unique data	4392	9929	10294
R_{int}	0.1955	0.0382	0.055
No. obs. Data ($I > 2\sigma(I)$)	2045	6101	7344
No. parameters	704	553	373
No. restraints	0	1	3
R_1 (obs data)	0.1251	0.0950	0.0779
wR_2 (all data)	0.3706	0.2583	0.2129
S	1.003	1.458	1.104

Supporting Information. Supporting information contains ^{1}H and ^{13}C NMR spectra, IR spectra, mass spectra, UV-vis spectra, maximum excitation and emission spectra, TRES measurements, and additional diagrams of crystal structures. This material is available free of charge via the Internet at http://pubs.acs.org. CCDC 1447801-1447803 contain the supplementary crystallographic data available free of charge via http://www.ccdc.cam.ac.uk/conts/retrieving.html, or from the Cambridge Crystallographic Data Centre, 12 Union Road, Cambridge CB2 1EZ, UK; fax (+44) 1223-336-033; or e-mail deposit@ccdc.cam.ac.uk.

Data Accessibility Data supporting this study are available within the supporting information and at http://doi.org/10.5518/65

Corresponding Authors

M.J. H. Email: m.j.hardie@leeds.ac.uk

M. P. C Email m.coogan@lancaster.ac.uk

Author Contributions

The manuscript was written through contributions of all authors. All authors have given approval to the final version of the manuscript.

The authors declare no competing financial interests.

Acknowledgments

This work was supported by the EPSRC through research grant EP/J001325/1, equipment grant EP/K039202/1 and through an EPSRC PhD studentship (VEP, DTG-2012). We thank Tanya Marinko-Covell at University of Leeds for elemental analyses, and Dr Lefteris Danos at University of Lancaster for assistance with time resolved spectroscopy.

References

1. Canceill, J.; Gabard, J.; Collet, A. *J. Chem. Soc., Chem. Commun.* **1983**, 122-123.

2. (a) Hardie, M. J. *Chem. Soc. Rev.* **2010**, *39*, 516-527; (b) Collet, A. *Tetrahedron* **1987**, *43*, 5725-5759.

3. for example (a) Huerta, E.; Isla, H.; Perez, E. M.; Bo, C.; Martin, N.; de Mendoza, J. *J. Am. Chem. Soc.* **2010**, *132*, 5351-5353; (b) Hiroshi, M.; Hasegawa, A.; Shiwaku, K.; Asano, K.; Uno, M.; Takahashi, S.; Yamamoto, K. *Chem. Lett.* **1998**, 923-924; (c) Steed, J. W.; Junk, P. C.; Atwood, J. A.; Barnes, M. J.; Raston, C. L.; Burkhalter, R. S. *J. Am. Chem. Soc.* **1994**, *116*, 10346-10347.

4. Wytko, J. A.; Boudon, C.; Weiss, J.; Gross, M. *Inorg. Chem.* **1996**, *35*, 4469-4477.

5. (a) Reynes, O.; Maillard, F.; Moutet, J.-C.; Royal, G.; Saint-Aman, E.; Stanciu, G.; Dutasta, J.-P.; Gosse, I.; Mulatier, J.-C. *J. Organomet. Chem.* **2001**, *637-639*, 356-363; (b) Holman, K. T.; Orr, G. W.; Atwood, J. L.; Steed, J. W. *Chem. Commun.* **1998**, 2109-2110.

6. Bohle, S. D.; Stasko, D. J. *Inorg. Chem.* **2000**, *39*, 5768-5770.

7. Carruthers, C.; Ronson, T. K.; Sumby, C. J.; Westcott, A.; Harding, L. P.; Prior, T. J.; Rizkallah, P.; Hardie, M. J. *Chem. Eur. J.* **2008**, *14*, 10286-10296.

8. Sumby, C. J.; Gordon, K. C.; Walsh, T. J.; Hardie, M. J. *Chem. Eur. J.* **2008**, *14*, 4415-4425.

9. Maiti, D.; Woertink, J. S.; Ghiladi, R. A.; Solomon, E. I.; Karlin, K. D. *Inorg. Chem.* **2009**, *48*, 8342-8356.

10. Holman, K. T.; Halihan, M. M.; Jurisson, S. S.; Atwood, J. L.; Burkhalter, R. S.; Mitchell, A. R.; Steed, J. W. *J. Am. Chem. Soc.* **1996**, *118*, 9567-9576.

11. (a) Coleman, A.; Brennan, C.; Vos, J. G.; Pryce, M. T. *Coord. Chem. Rev.* **2008**, *252,* 2585–2595; (b) Stufkens, D. J.; Vlček, A. Jr. *Coord. Chem. Rev.* **1998**, *177*, 127-179.

12. Beer, P. D.; Hayes, E. J. *Coord. Chem. Rev.* **2003**, *240,*167-189.

13. Thanasekaran, P.; Lee, C.-C.; Lu, K.-L. Acc. Chem. Res. **2012**, 45, 1403-1418.

14. Fernández-Moreira, V.; Thorp-Greenwood, F. L.; Coogan, M. P. *Chem. Commun.* **2010**, *46*, 186-202.

15. Michalet, X.; Pinaud, F. F.; Bentolila, L. A.; Tsay, J. M.; Doose, S.; Li, J. J.; Sundaresan, G.; Wu, A. M.; Gambhir, S. S.; Weiss, S. *Science* **2005**, *307*, 538-544.

16. Botchway, S. W.; Charnley, M.; Haycock, J. W.; Parker, A. W.; Rochester, D. L.; Weinstein, J. A.; Williams, J. A. G. *Proc. Natl. Acad. Sci. U. S. A.* **2008**, *105*, 16071-16076.

17. Stucker, M.; Schulze, L.; Pott, G.; Hartmann, P.; Lubbers, D. W.; Rochling, A.; Altmeyer, P. *Sens. Actuators* **1998**, *51*, 171-175.

18. Haino, T.; Araki, H.; Fujiwara, Y.; Tanimoto, Y.; Fukazawa, Y. Chem. Commun. **2002**, 2148-2149.

19. (a) Beer, P. D.; Cooper, J. B. Chem. Commun. **1998**, 129-130; (b) Beer, P. D.; Drew, M. G. B.; Hesek, D.; Shade, M.; Szemes, F. Chem. Commun. **1996**, 2161-2162.

20. Beer, P. D.; Timoshenko, V.; Maestri, M.; Passaniti, P.; Balzani, V. Chem. Commun. **1999**, 1755-1756.

21. Hissler, M.; Harriman, A.; Jost, P.; Wipff, G.; Ziessel, R. Angew. Chem. Int. Ed. **1998**, 37, 3249-3252.

22. (a) Busi, M.; Cantadori, B.; Boccini, F.; De Zorzi, R.; Geremia, S.; Dalcanale, E. Eur. J. Org. Chem. **2011**, 2629-2642; (b) Menozzi, E.; Busi, M.; Ramingo, R.; Campagnolo, M.; Geremia, S.; Dalcanale, E. Chem. Eur. J. **2005**, 11, 3136-3148.

23. Botana, E.; Da Silva, E.; Benet-Buchholz, J.; Ballester, P.; de Mendoza, J. Angew. Chem. Int. Ed. **2007**, 46, 198-201.

24. (a) Laramée-Milette, B.; Lachance-Brais, C.; Hanan G. S. Dalton Trans. **2015**, 44, 41-45; (b) Nagarajaprakash, R.; Divya, D.; Ramakrishna, B.; Manimaran, B. Organometallics **2014**, 33, 1367-1373; (c) Shankar, B.; Elumalai, P.; Sathiyashivan, S. D.; Sathiyendiran, M. Inorg. Chem.

2014, 53, 10018-10020; (d) Shankar, B.; Hussain, F.; Sathiyendiran, M. J. Organomet. Chem. **2012**, 725, 26-29; (e) Coogan, M. P.; Fernández-Moreira, V.; Kariuki, B. M.; Pope, S. J. A.; Thorp-Greenwood, F. L. Angew. Chem. Int. Ed. **2009**, 48, 4965-4968.

25. Westcott A.; Fisher J.; Harding L. P.; Rizkallah P.; Hardie M. J. *J. Am. Chem. Soc.*, **2008**, *130*, 2950-2951.

26. for example (a) Fernandez-Moreira, V.; Thorp-Greenwood, F. L.; Arthur, R. J.; Kariuki, B. M.; Jenkins, R. L.; Coogan, M. P. *Dalton Trans.* **2010**, *39*, 7493-7503; (b) Metcalfe, C.; Spey, S.; Adams, H.; Thomas, J. A. *J. Chem. Soc., Dalton Trans.* **2002**, 4732-4739; (c) Moya, S. A.; Pastene, R.; Le Bozec, H.; Baricelli, P. J.; Pardey, A. J.; Gimeno, J. *Inorg, Chim. Acta* **2001**, *312*, 7-14; (d) Abel, E. W; Dimitrov, V. S.; Long, N. J.; Orrell, K. G.; Osborne, A. G.; Pain, H. M.; Šik, V.; Hursthouse, M. B.; Mazid, M. A. *J. Chem. Soc., Dalton Trans.* **1993**, 597-603.

27. Steed, J. W.; Zhang, H.; Atwood, J. L. *Supramol. Chem.* **1996**, *7*, 37-45.

28. (a) Henkelis, J. J.; Barnett, S. A.; Harding, L. P.; Hardie, M. J. *Inorg. Chem.* **2012**, 10657-10674; (b) Ronson, T. K.; Carruthers, C.; Fisher, J.; Brotin, T.; Harding, L. P.; Rizkallah, P. J.; Hardie, M. J. *Inorg. Chem.* **2010**, *49*, 675-685; (c) Hardie, M. J.; Mills, R. M.; Sumby, C. J. *Org. Biomol. Chem.* **2004**, *2*, 2958-2964.

29. (a) Little, M. A.; Donkin, J.; Fisher, J.; Halcrow, M. A.; Loder, J.; Hardie, M. J. *Angew. Chem. Int. Ed.* **2012**, *51*, 764-766; (c) Givelet, C.; Sun, J.; Xu, D.; Emge, T. J.; Dhokte, A.; Warmuth, R. *Chem. Commun.* **2011**, *47*, 4511-4513; (d) Makita, Y.; Sugimoto, K.; Furuyoshi, K.; Ikeda, K.; Fujita, T.; Fujiwara, S.-I.; Ogawa, A. *Supramol. Chem.* **2011**, *23*, 269-272.

30. (a) Yin Zhang, K.; Ka-Shum, T. K.; Louie, M.-W.; Liu, H.-W.; Kam-Wing Lo, K. *Organometallics* **2013**, *32*, 5098-5102; (b) Bertrand, H. C.; Clède, S.; Guillot, R.; Lambert, F.; Policar, C. *Inorg. Chem.* **2014**, *53*, 6204-6223; (c) Fernández-Moreira, V.; Ortego, M. L.; Williams, C. F.; Coogan, M. P.; Villacampa, M. D.; Gimeno, M. C. *Organometallics* **2012***, 31*, 5950-5957.

31. (a) Lo, K. K.-W.; Zhang, K. Y.; Leung, S.-K.; Tang, M.-C. *Angew. Chem., Int. Ed.*, **2008**, *47*, 2213-2216; (b) Glazer, E. C.; Magde, C.; Tor, Y. *J. Am. Chem. Soc.* **2005**, *127*, 4190-4192 ; (c) Keyes, T. E. *Chem. Commun.* **1998**, 889-894.

32. Marsh, J. K. *J. Chem. Soc. Trans.*, **1924**, *125*, 418-423.

33. Henry, M. S.; Hoffman, M. Z. *J. Phys. Chem*. **1979**, *83*, 618-625.

34. Kasha M. *Discuss. Faraday Soc.*, **1950**, *9*, 14-19.

35. Feng Y.; Cheng J.; Zhou L.; Xhou X.; Xiang H. *Analyst*, **2012**, *137*, 4885-4901.

36. Lin, R-J.; Chang, I-Jy.; *J. Chin. Chem. Soc.* **2002,** *49*, 161-164.

37. Pope, S. J. A.; Coe, B. J.; Faulkner, S. *Chem Commun.* **2004**, 1550-1551.

38. (a) Scott, J. L.; MacFarlane, D. R.; Raston, C. L.; Teoh, C. M. *Green Chem.* **2000**, *2*, 123-126; (b) Canceill, J.; Collet, A.; Gottarelli, G. *J. Am. Chem. Soc.* **1984**, *106*, 5997-6003.

39. Sheldrick, G. M. *Acta Cryst.* **2008**, *A64,* 112-122.

40. Spek, A. L. *Acta Cryst.*, **1990**, *A46*, C34

Insert Table of Contents Graphic and Synopsis Here

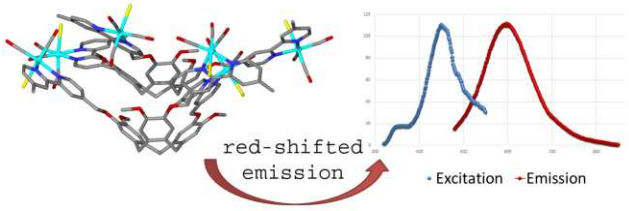

Three novel trimetallic rhenium *fac*-tricarbonylbromide complexes have been synthesised coordinated to cavitand ligands decorated with bipyridine or terpyridine groups. These complexes show red-shifted emission wavelengths compared with those typical of monometallic $Re(CO)_3$-bipy-Br complexes and some show an unusual dual-emission phenomenon.